



Published in final edited form as:

*Biochem Biophys Res Commun.* 2008 January 4; 365(1): 42–46.

## Effect of heterodimer partner RXR $\alpha$ on PPAR $\gamma$ activation function-2 helix in solution

Jianyun Lu<sup>a,\*</sup>, Minghe Chen<sup>a</sup>, Susan E. Stanley<sup>a</sup>, and Ellen Li<sup>a,b</sup>

<sup>a</sup> Department of Internal Medicine, Washington University School of Medicine, St. Louis, MO 63110

<sup>b</sup> Department of Biochemistry and Molecular Biophysics, Washington University School of Medicine, St. Louis, MO 63110

### Abstract

The structural mechanism of allosteric communication between retinoid X receptor (RXR) and its heterodimer partners remains controversial. As a first step towards addressing this question, we report a nuclear magnetic resonance (NMR) study on the GW1929-bound peroxisome proliferator-activated receptor gamma (PPAR $\gamma$ ) ligand-binding domain (LBD) with and without the 9-cis-retinoic acid (9cRA)-bound RXR $\alpha$  LBD. Sequence-specific <sup>13</sup>C $\alpha$ , <sup>13</sup>C $\beta$  and <sup>13</sup>CO resonance assignments have been established for over 95% of the 275 residues in the PPAR $\gamma$  LBD monomer. The <sup>1</sup>HN, <sup>15</sup>N and <sup>13</sup>CO chemical shift perturbations induced by the RXR LBD binding are located at not only the heterodimer interface that includes the C-terminal residue Y477, but also residues Y473 and K474 in the activation function-2 (AF-2) helix. This result suggests that 9cRA-bound RXR $\alpha$  can affect the PPAR $\gamma$  AF-2 helix in solution, and demonstrates that NMR is a powerful new tool for studying the mechanism of allosteric ligand activation in RXR heterodimers.

### Keywords

PPAR $\gamma$ ; RXR $\alpha$ ; Heterodimer; Activation; Allosteric communication; NMR

### Introduction

Retinoid X receptors (RXR $\alpha$ ,  $\beta$ ,  $\gamma$ ) are members of the nuclear receptor (NR) superfamily of ligand-activated transcription factors that bind to DNA response elements as either homodimers or obligate heterodimer partners with several other nuclear receptors [1] such as peroxisome proliferator-activated receptors (PPAR $\alpha$ ,  $\beta/\delta$ ,  $\gamma$ ). Both RXR and PPAR consist of an N-terminal A/B domain that contains a ligand-independent activation function-1, a conserved DNA-binding domain, a flexible hinge or D domain, and a ligand-binding domain (LBD) that contains a ligand-dependent activation function-2 (AF-2) at its C-terminal region and a dimerization interface.

PPARs are permissive RXR heterodimer partners so that a RXR agonist can either activate the heterodimer alone or potentiate PPAR agonist activation. Whether allosteric communication across the heterodimer interface facilitates the allosteric ligand activation remains

\*Corresponding author. Fax: 1-314-362-8959. E-mail: lujy@wustl.edu.

**Publisher's Disclaimer:** This is a PDF file of an unedited manuscript that has been accepted for publication. As a service to our customers we are providing this early version of the manuscript. The manuscript will undergo copyediting, typesetting, and review of the resulting proof before it is published in its final citable form. Please note that during the production process errors may be discovered which could affect the content, and all legal disclaimers that apply to the journal pertain.

controversial, as reported in the crystallographic studies on the estrogen receptor LBD homodimer [2] and retinoic acid receptor-RXR LBD heterodimer [3].

To address this question, we initiated a nuclear magnetic resonance (NMR) study on the agonist GW1929-bound PPAR $\gamma$  LBD with and without the agonist 9-cis-retinoic acid (9cRA)-bound RXR $\alpha$  LBD. Our result suggests that 9cRA-bound RXR $\alpha$  can affect the PPAR $\gamma$  AF-2 helix in solution through the C-terminal residue Y477 at the interface, and demonstrates, for the first time, that NMR is a powerful new tool for studying the mechanism of allosteric ligand activation in RXR heterodimers.

## Materials and Methods

### Materials

The PPAR $\gamma$  ligand GW1929 and RXR $\alpha$  ligand 9cRA were purchased from Sigma-Aldrich (St. Louis, MO). The PPAR $\gamma$  LBD (a.a. Q203-Y477) cDNA was amplified from human adipose cDNA library and inserted at the *NdeI/XhoI* restriction sites of the pET15b expression vector as described [4]. DNA sequencing analysis confirmed the pET15b-PPAR $\gamma$  LBD sequence. The unlabeled RXR $\alpha$  LBD, PPAR $\gamma$  LBD and U-[<sup>2</sup>H, <sup>15</sup>N, <sup>13</sup>C]-enriched PPAR $\gamma$  LBD were expressed in *Escherichia coli* BL21-DE3 bacteria, isolated by Talon affinity chromatography, digested by thrombin to remove the N-terminal His<sub>6</sub> tag, and finally purified by gel filtration chromatography as described [4].

### Fluorescence Titration

Experiments were performed on 2.25 ml of 1  $\mu$ M unlabeled PPAR $\gamma$  LBD in gel filtration buffer (50 mM NaCl, 10 mM Tris, pH 8.0, 0.5 mM EDTA, and 10 mM  $\beta$ -mercaptoethanol) containing 0.01% gelatin at 25°C using a fluorometer (Photon Technology International, Birmingham, NJ) by exciting tyrosine residues at 280 nm and monitoring their fluorescence emission at 308 nm before and after adding aliquots (0.4  $\mu$ l) of 240  $\mu$ M GW1929 dimethyl sulfoxide solution, as described [5]. To evaluate inner filter effect, experiments were performed on ~1  $\mu$ M L-tyrosine under the same conditions. Correction for inner filter effect and calculation of the  $K_d$  were carried out as described [6]. The reported  $K_d$  was the average over three independent measurements.

### NMR Sample Preparation

The unliganded PPAR $\gamma$ -RXR $\alpha$  heterodimer was prepared by mixing equal molar amounts of the purified LBDs and adjusting to a 1:1 molar ratio according to the gel filtration chromatogram of the complex. A NMR sample containing 0.27 mM unliganded (apo), labeled PPAR $\gamma$  LBD monomer, 1.0 mM GW1929-bound, labeled PPAR $\gamma$  LBD monomer, or 1.0 mM heterodimer of GW1929-bound, labeled PPAR $\gamma$  LBD with 9cRA-bound, unlabeled RXR $\alpha$  LBD in a NMR buffer (20 mM potassium phosphate, pH 7.4, 50 mM KCl, 0.05% NaN<sub>3</sub>, 0.5 mM EDTA-*d*<sub>16</sub>, 8 mM  $\beta$ -mercaptoethanol- *d*<sub>6</sub> and 5% D<sub>2</sub>O) was prepared as described [4].

### NMR Spectroscopy

Experiments were conducted at 25°C in either a 600- or 700-MHz four-channel Varian Inova spectrometer equipped with a pulsed-field gradient triple resonance probe. For sequence-specific resonance assignments, a 2-dimensional (2D) <sup>1</sup>H-<sup>15</sup>N-heteronuclear single quantum correlation (HSQC) spectrum and six 3D- and 4D-triple resonance through-bond experiments were performed on the 1.0 mM liganded PPAR $\gamma$  LBD monomer sample as described [4]. For analyzing the chemical shift perturbation induced by heterodimerization with the liganded RXR $\alpha$  LBD, 2D HSQC and 3D HNCQ experiments were performed on the 1.0 mM heterodimer sample. Details on the experimental parameters, data processing and chemical

shift-derived secondary structure were as described [4]. The weighted root-mean-squared deviation of chemical shifts between the monomer and heterodimer was defined as:  $\Delta\delta_{\text{RMSD}} = \sqrt{(\Delta\delta_{\text{HN}})^2 + (0.154\Delta\delta_{\text{N}})^2 + (0.341\Delta\delta_{\text{CO}})^2}$  [7].

## Results

The PPAR $\gamma$  LBD was purified as monomer to more than 95% chemical homogeneity by gel filtration chromatography. The dissociation constant  $K_d$  of GW1929 binding to the PPAR $\gamma$  LBD was  $19 \pm 10$  nM by fluorescence titration. This value was similar to the reported half-maximal activation  $EC_{50}$  of  $9 \pm 7$  nM for GW1929 [8], suggesting that the purified PPAR $\gamma$  LBD was functional. The gel filtration chromatography of a heterodimer sample and the subsequent SDS-PAGE analysis of the elution fractions showed that the two LBDs were co-eluted in a 1:1 molar ratio (Supplementary Fig. 1), suggesting that the heterodimer (59.0 kDa) was predominant over the PPAR $\gamma$  LBD monomer (31.8 kDa) and RXR $\alpha$  LBD homodimer (54.4 kDa).

Sequence-specific  $^{13}\text{C}^\alpha$ ,  $^{13}\text{CO}$  and  $^{13}\text{C}^\beta$  resonance assignments have been established for 262 of the 275 residues (> 95%) in the GW1929-bound PPAR $\gamma$  LBD monomer using a previously described method [4]. The chemical shift values are listed in Supplementary Table 1 and have been deposited in BioMagResBank with accession number BMRB15518. The 2D-HSQC spectra of the apo- and liganded-LBD are shown in Fig. 1. The backbone amide crosspeaks of 244 residues (> 92%) have been identified from a total of 264 expected residues after excluding the 11-proline residues in the liganded-LBD. In contrast, at least 62 backbone amide crosspeaks were missing in the 2D-HSQC spectrum of the apo-LBD sample, including those in the AF-2 helix and the C-terminal region. This result suggests that GW1929 binding stabilizes the PPAR $\gamma$  LBD conformation.

The  $^{13}\text{C}^\alpha$ ,  $^{13}\text{CO}$  and  $^{13}\text{C}^\beta$  chemical shift deviations from the random coil values after correction for the deuterium isotope effect [4] and the secondary structure determined by the chemical shift index (CSI) program [9] are shown in Fig. 2. The CSI consensus reveals that the PPAR $\gamma$  LBD has 12  $\alpha$ -helices, which match those in the crystal structure of the PPAR $\gamma$  LBD bound to GI262570 (farglitazar) and a coactivator peptide [10] and are usually shortened by up to one turn on either end of the helix except for helices H2', H3 and H8. The analysis of helices H3 and H8 may be affected by the missing resonance assignments and helix H3', which is not part of the canonical NR LBD structure, is not detected here either. Although the CSI consensus reveals only one  $\beta$ -strand S4, the  $^{13}\text{C}^\alpha$  chemical shift changes support the existence of  $\beta$ -strands S2 and S3 but not S1.

To examine the effect of heterodimerization and RXR ligand binding on the PPAR $\gamma$  LBD, we analyzed crosspeak displacements between the monomer and heterodimer in the 2D-HSQC and 3D-HNCO spectra, as shown in Fig. 3A and 3B. Using  $\Delta\delta_{\text{RMSD}} = 0.13$  ppm as the cutoff, which corresponds to  $\Delta\delta_{\text{HN}} = 0.05$  ppm,  $\Delta\delta_{\text{N}} = 0.4$  ppm and  $\Delta\delta_{\text{CO}} = 0.3$  ppm, or  $\Delta\delta_{\text{RMSD}} = 0.08$  ppm when  $\Delta\delta_{\text{CO}}$  is excluded due to unavailable  $^{13}\text{CO}$  resonance assignment in the heterodimer, we mapped residues with chemical shift perturbations above and below the cutoff in red (moderate) and blue (small), respectively, on the crystal structure [10], as shown in Fig. 3C. The red residues are primarily located in H9 and H10, the H8-H9 and H9-H10 loops and the C-terminal residue Y477, all of which are components of the heterodimer interface. Residues Y320 in H4 and E324 in H5 (Fig. 3A) that are sequentially remote from the interface are also red. A close inspection of the crystal structure reveals that these two residues and other six residues including R397 (Fig. 3A) in the H8-H9 loop, R443, V446, T447 and V450 in H10, and L476 in the C-terminal region are in close contact ( $\leq 4.2$  Å) with Y477 (Fig. 3D). Consistently, all eight residues are red upon heterodimerization. Intriguingly, residues Y473

(Fig. 3B) and K474 in the AF-2 helix are also red, suggesting that 9cRA-bound RXR $\alpha$  can affect the PPAR $\gamma$  AF-2 helix in solution.

## Discussion

In this study, we have established sequence-specific  $^{13}\text{C}^\alpha$ ,  $^{13}\text{C}^\beta$  and  $^{13}\text{CO}$  resonance assignments for over 95% of the 275 residues in the GW1929-bound PPAR $\gamma$  LBD monomer. The chemical shift-derived secondary structure generally agrees with the crystal structure of the PPAR $\gamma$  LBD-GI262570-coactivator peptide ternary complex [10]. Both GW1929 [8] and GI262570 [10] are N-aryl tyrosine derivatives that were designed to mimic the interactions between the PPAR $\gamma$  H3, H5, H10 and AF-2 helices and the insulin-sensitizing thiazolidinedione (TZD) drug rosiglitazone head group in the crystal structure [11]. Previous NMR study [12] on the PPAR $\gamma$  LBD without (apo) and with rosiglitazone binding showed that the 3D HNCOC spectra of the apo-LBD had less than half of the expected crosspeaks, and rosiglitazone binding restored the missing crosspeaks including those in the AF-2 helix and the C-terminus Y477. This is similar to our finding on GW1929 binding to the PPAR $\gamma$  LBD. Therefore, both NMR studies support the crystallographic findings that both rosiglitazone and N-aryl tyrosine directly interact with the AF-2 helix.

Our chemical shift perturbation analysis shows that heterodimerization with 9cRA-bound RXR causes moderate backbone  $^1\text{HN}$ ,  $^{15}\text{N}$  and  $^{13}\text{CO}$  chemical shift changes of the PPAR $\gamma$  LBD in areas that generally coincide with the heterodimer interface in the crystal structure, and in residues that are in close contact with the C-terminus Y477. Intriguingly, residues Y473 and K474 in the AF-2 helix also exhibit moderate chemical shift changes. This is unexpected from the crystal structures because the conformations of the AF-2 helix H12 and the C-terminal segment D475-L476 in both homodimer [13] and heterodimer [10] configurations are very similar (Fig. 3E). The results from gel filtration chromatography and NMR lineshape analysis suggest that the PPAR $\gamma$  LBD is mainly a monomer in solution regardless of ligand binding. The chemical shift perturbation on the AF-2 helix could be the result of the displacement of the Y477 side chain, a small backbone conformational change in the segment Y473-Y477 or both, the latter of which would affect ligand-dependent PPAR $\gamma$  activation. Further NMR and mutational studies should determine the precise structural mechanism. A parallel study on the RXR $\alpha$  LBD subunit should identify other structural determinants of allosteric ligand activation.

Finally, we demonstrate, for the first time, that it is feasible to monitor residue-specific structural and dynamic changes of a RXR LBD heterodimer in response to ligand binding in solution, and NMR is a powerful new tool for studying the mechanism of allosteric ligand activation in RXR heterodimers.

## Supplementary Material

Refer to Web version on PubMed Central for supplementary material.

### Acknowledgements

This work was supported by grants from the National Institutes of Health (NIH) DK59501 (E. Li), Washington University Digestive Diseases Research Core Center (DK 52574), a pilot/feasibility award (J. Lu) from the Washington University Center for Human Nutrition (DK 56341). We thank Mr. Weidong Wen for preparing human adipose cDNA library and Mr. Bob McGibbon for assistance in protein purification.

## References

1. Mangelsdorf DJ, Evans RM. The RXR heterodimers and orphan receptors. *Cell* 1995;83:841–850. [PubMed: 8521508]

2. Nettles KW, Sun J, Radek JT, Sheng S, Rodriguez AL, Katzenellenbogen JA, Katzenellenbogen BS, Greene GL. Allosteric control of ligand selectivity between estrogen receptors  $\alpha$  and  $\beta$ : implications for other nuclear receptors. *Mol Cell* 2004;13:317–327. [PubMed: 14967140]
3. Pogenberg V, Guichou JF, Vivat-Hannah V, Kammerer S, Perez E, Germain P, de Lera AR, Gronemeyer H, Royer CA, Bourguet W. Characterization of the interaction between retinoic acid receptor/retinoid X receptor (RAR/RXR) heterodimers and transcriptional coactivators through structural and fluorescence anisotropy studies. *J Biol Chem* 2005;280:1621–633.
4. Lu J, Cistola DP, Li E. Analysis of ligand binding and protein dynamics of human retinoid X receptor alpha ligand-binding domain by nuclear magnetic resonance. *Biochemistry* 2006;45:1629–1639. [PubMed: 16460010]
5. Cheng L, Norris AW, Tate BF, Rosenberger M, Grippo JF, Li E. Characterization of the ligand binding domain of human retinoid x receptor  $\alpha$  expressed in *Escherichia coli*. *J Biol Chem* 1994;269:18662–18667. [PubMed: 8034615]
6. Norris AW, Li E. Fluorometric titration of the CRABPs. *Methods Mol Biol* 1998;89:123–139. [PubMed: 9664324]
7. Tugarinov V, Kay LE. Quantitative NMR studies of high molecular weight proteins: application to domain orientation and ligand binding in the 723 residue enzyme malate synthase G. *J Mol Biol* 2003;327:1121–1133. [PubMed: 12662935]
8. Brown KK, Henke BR, Blanchard SG, Cobb JE, Mook R, Kaldor I, Kliewer SA, Lehmann JM, Lenhard JM, Harrington WW, Novak PJ, Faison W, Binz JG, Hashim MA, Oliver WO, Brown HR, Parks DJ, Plunket KD, Tong WQ, Menius JA, Adkison K, Noble SA, Willson TM. A novel N-aryl tyrosine activator of peroxisome proliferator-activated receptor- $\gamma$  reverses the diabetic phenotype of the Zucker diabetic fatty rat. *Diabetes* 1999;48:1415–1424. [PubMed: 10389847]
9. Wishart DS, Sykes BD. The  $^{13}\text{C}$  chemical-shift index: a simple method for the identification of protein secondary structure using  $^{13}\text{C}$  chemical-shift data. *J Biomol NMR* 1994;4:171–180. [PubMed: 8019132]
10. Gampe RT Jr, Montana VG, Lambert MH, Miller AB, Bledsoe RK, Milburn MV, Kliewer SA, Willson TM, Xu HE. Asymmetry in the PPAR $\gamma$ /RXR $\alpha$  crystal structure reveals the molecular basis of heterodimerization among nuclear receptors. *Mol Cell* 2000;5:545–555. [PubMed: 10882139]
11. Nolte RT, Wisely GB, Westin S, Cobb JE, Lambert MH, Kurokawa R, Rosenfeld MG, Willson TM, Glass CK, Milburn MV. Ligand binding and co-activator assembly of the peroxisome proliferator-activated receptor- $\gamma$ . *Nature* 1998;395:137–143. [PubMed: 9744270]
12. Johnson BA, Wilson EM, Li Y, Moller DE, Smith RG, Zhou G. Ligand-induced stabilization of PPAR $\gamma$  monitored by NMR spectroscopy: implications for nuclear receptor activation. *J Mol Biol* 2000;298:187–194. [PubMed: 10764590]
13. Cronet P, Petersen JFW, Folmer R, Blomberg N, Sjoblom K, Karlsson U, Lindstedt EL, Bamberg K. Structure of the PPAR $\alpha$  and - $\gamma$  ligand binding domain in complex with AZ 242; ligand selectivity and agonist activation in the PPAR family. *Structure* 2001;9:699–706. [PubMed: 11587644]

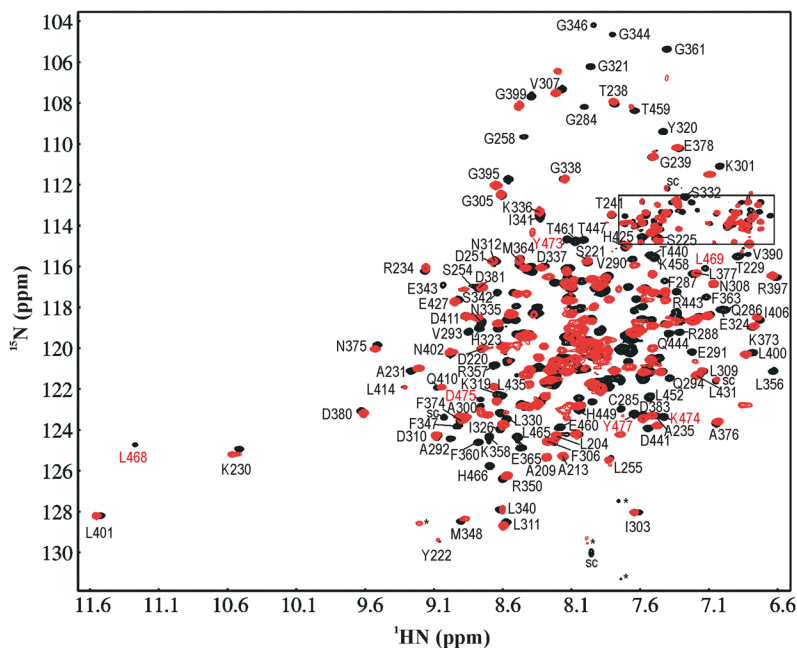


**Fig. 1.** GW1929 binding stabilizes the PPAR $\gamma$  LBD conformation. The 2D-HSQC spectrum of a 0.27 mM apo-PPAR $\gamma$  LBD sample (red) was superimposed onto that of a 1.0 mM GW1929-bound PPAR $\gamma$  LBD sample (black). Crosspeaks in less crowded regions of the GW1929-bound PPAR $\gamma$  LBD sample are labeled with the amino acid one-letter code and the residue number. All labels are black except for those in the AF-2 helix and the C-terminal region (red). Side chain crosspeaks are either enclosed in a box or labeled with “sc”. Asterisks designate unknown crosspeaks, most of which are likely from minor aggregates.

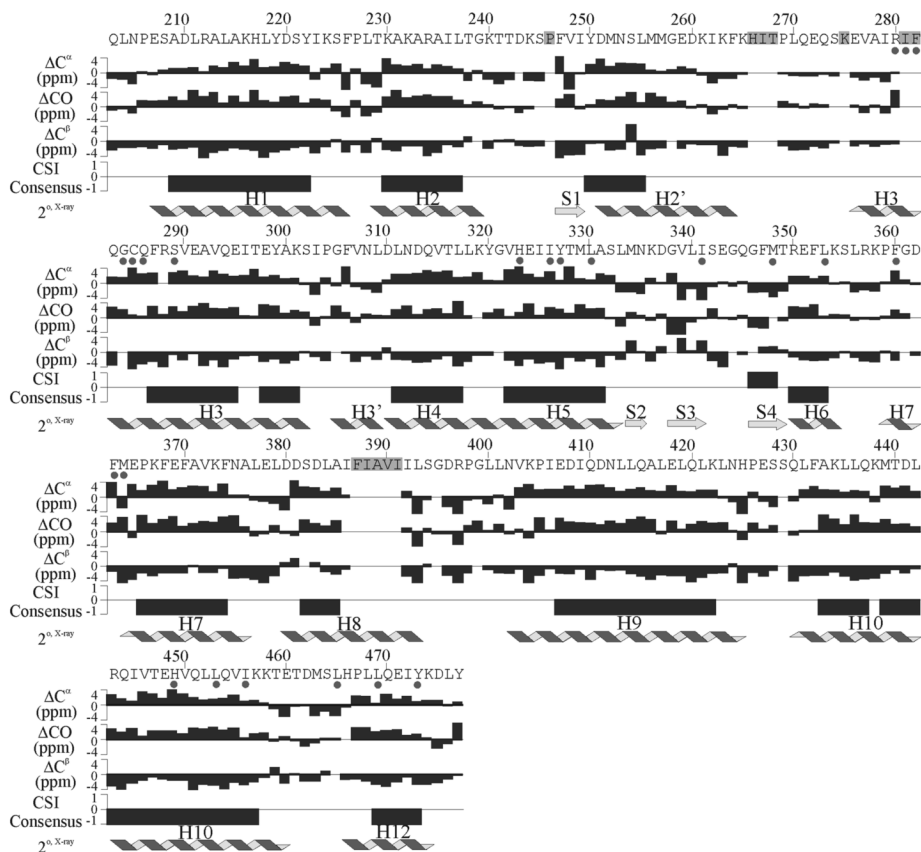


**Fig. 2.** Chemical shift-derived secondary structure of GW1929-bound PPAR $\gamma$  LBD monomer. The  $^{13}C^{\alpha}$ ,  $^{13}CO$  and  $^{13}C^{\beta}$  chemical shift deviations between the measured and random coil values and the chemical shift index (CSI) consensus are plotted versus the primary sequence at the top. The three CSI values 1, 0 and -1 designate  $\alpha$ -helix (H1-H12), random coil and  $\beta$ -sheet (S1-S4), respectively. The ribbon diagrams depict the secondary structure in the crystal structure of the PPAR $\gamma$  LBD-GI262570-coactivator peptide ternary complex (PDB: 1FM9). The primary sequence is annotated as followed: the shaded letters are unassigned residues; filled circles are residues in close contact ( $\leq 4.2 \text{ \AA}$ ) with GI262570.

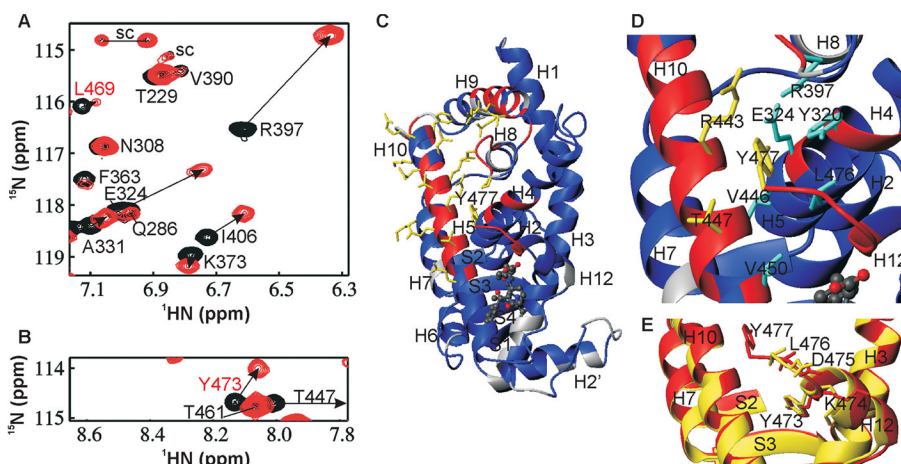


**Fig. 3.** Chemical shift perturbation induced by heterodimer partner 9cRA-bound RXR $\alpha$ LBD. (A), (B) Overlays of the expanded regions in the 2D-HSQC spectra recorded on either 1.0 mM GW1929-bound PPAR $\gamma$  LBD monomer (black) or its heterodimer with 9cRA-bound and unlabeled RXR $\alpha$  LBD (red). The annotation is the same as that described in Fig. 1, with arrows indicating crosspeak displacement. (C) Chemical shift perturbation mapping on the crystal structure of the PPAR $\gamma$  LBD-GI262570 (ball-and-stick model with C, N and O atoms in dark, blue and red, respectively)-coactivator peptide (not shown) ternary complex. Color schemes: red and blue, moderate and small chemical shift changes, respectively; gray, proline residues and unassigned residues in either monomer or heterodimer; yellow, side chains of residues at the heterodimer interface. (D) Zooming onto the C-terminal residue Y477 and the eight residues in close contact with it. The side chains outside the heterodimer interface are in light blue. (E) Superimposition of the crystal structure (PDB: 1I7I) of the AZ242-bound PPAR $\gamma$  LBD homodimer (yellow) onto that of the PPAR $\gamma$ -RXR $\alpha$  LBD heterodimer (red) bound to ligands (GI262570 and 9cRA) and coactivator peptides showing the similarity between the two AF-2 helices. Residue Y477 is missing in the crystal structure of the homodimer. Helices H2', H4 and H5 have been removed for clarity.